

Metal-Anion Coordination and Linker-Anion Hydrogen Bonding in the Construction of Metal-Organic Frameworks from Bipyrazole

Erpan Zhang,^{*,a} Qizhang Jia,^b Jun Zhang,^a and Zhenguo Ji^a

^a College of Materials and Environmental Engineering, Hangzhou Dianzi University, Hangzhou, Zhejiang 310018, China

^b Department of Chemistry, Fudan University, Shanghai 200433, China

Two new two-dimensional frameworks based on packing of square grids, Cu(Me₄bpz)₂(NO₃)₂ (**1**) and Zn(Me₄bpz)(SO₄) (**2**) (Me₄bpz=3,3',5,5'-tetramethyl-4,4'-bipyrazole), have been synthesized by mild solvothermal method. In addition to the major metal-organic linker coordination, they allow us to study how the metal-inorganic anion coordination and organic linker-inorganic anion hydrogen bonding affect the resulting structures during the framework assembly.

Keywords metal-organic frameworks, nitrogen-containing heterocycle, solvothermal synthesis, crystal structure

Introduction

Metal-organic frameworks (MOFs)^[1-8] are porous crystalline structures constructed from inorganic nodes and organic linkers. Here, the multi-topic organic ligands are usually polycarboxylic acids and heterocycles, and the inorganic nodes are metal ions or clusters. In several cases, inorganic anions, such as Cl⁻, NO₃⁻, and SO₄²⁻ from metal salts, also coordinate to the metal ions, acting as terminal ligands or bridging linkers in the MOF assembly. This scenario is observed more frequently when N-based ligands are used as linkers, for the reasons that i) this coordination is based on the lone pairs from a neutral ligand, as in the pyridine case; and ii) the hydrogen atom in the protonated N-H could not be removed in the reaction conditions applied, as in the imidazole case. In both cases, it is natural for the inorganic ions to stay in the framework structures to maintain the electric neutrality of the structure. On the other hand, as for the self-assemblies of MOFs, the geometries of organic ligands and inorganic secondary building units (SBUs)^[9] are the key factors which determine the topologies of the final structures. The presence of inorganic anions will obviously affect the coordination environment of the metal ions, and thus results in a number of different crystal structures.^[10]

In the past few years, several MOFs consisting of 3,3',5,5'-tetramethyl-4,4'-bipyrazole (Me₄bpz) have been reported.^[11-28] Me₄bpz is highly flexible due to that the two pyrazole rings can rotate around the central C-C

bond, and a wide angle of 50°–90° between the two pyrazole rings were observed in the MOFs based on Me₄bpz. Previous calculations have demonstrated that the relative energies of the conformers are very similar ($\Delta E = 0.92, 3.89, 11.02$, and 27.17 kJ/mol for 70°, 60°, 45°, and 30°, respectively),^[27,28] which makes diverse range of coordination assemblies available. What is more, like many linkers based on heterocycles, Me₄bpz can either act as a neutral bridging linker by using both pyrazole ends to ligate two metal ions, or serve as anionic and tetradeinate ligand to bridge four metal ions, depending on the protonated or deprotonated pyrazolate N-H groups. Obviously, different reaction conditions, such as solvents, metal sources, temperature, and pH, can lead to different MOFs structures.^[29] Usually, deprotonation of pyrazolate N-H groups is deeply related to the reaction parameters applied. Relatively high energy or basicity is needed to remove the hydrogen atoms from N-H groups, while a mild reaction condition is beneficial to retain the hydrogen atoms. In addition, Me₄bpz possesses effective hydrogen bond donor (N-H) for the formation of hydrogen bond. The hydrogen bond between the linker and the anion or solvent greatly affects the conformation of the linker, resulting in MOFs with different structures.

Herein, by using the methyl functionalized bipyrazole ligand Me₄bpz, two new MOF structures, where the pyrazoles were still protonated, have been constructed. Both structure **1** [Cu(Me₄bpz)₂(NO₃)₂] and structure **2** [Zn(Me₄bpz)₂SO₄] show layered structure, and the lay-

* E-mail: epzhang@hdu.edu.cn; Tel.: 0086-0571-86878609

Received September 5, 2015; accepted November 11, 2015; published online December 15, 2015.

Supporting information for this article is available on the WWW under <http://dx.doi.org/10.1002/cjoc.201500640> or from the author.

ers are further packed in an eclipsed form to form 1D channels. Specifically, NO_3^- and SO_4^{2-} from metal salts have participated in the assembly of the networks. Due to the different coordination modes of the anions, the monodentate NO_3^- and the bidentate SO_4^{2-} have created single metal ions (as in structure **1**) and metal clusters (in structure **2**) as inorganic SBUs for the MOFs. What is more, the anions are also involved in the hydrogen bonding with the linkers. The *endo*-conformation of the linker is preferred due to the hydrogen bonding, which has further tuned the MOF structures. These two MOFs provide examples of metal-inorganic anion coordination and organic linker-inorganic anion hydrogen bonding in the extended structures. Compared with the major metal-linker coordination in the MOF assembly, these interactions provide interesting ways to further control the resulting structures.

Experimental

Synthesis

Me₄bpz All chemicals were of reagent grade quality obtained from commercial sources and used without further purification. Me₄bpz was synthesized by following the literature method.^[30,31] 2,4-Pentanedione (10.0 g, 11.0 mL) and NaH (4.0 g) were added to Et₂O (200 mL) under the protection of N₂ with continuously stirring. Soxhlet extraction was performed four times with I₂ (12.0 g) to obtain intermediate **a** (see Scheme S1 in the Supporting Information). After **a** was recrystallized with CH₃OH, N₂H₄•H₂O (6.0 mL) and water (5.0 mL) were mixed with 5.7 g **a**, and the mixture was stirred at room temperature for 2 h. Finally, the filtered precipitates were dissolved in CH₃OH, and the filtrate were rotavaped to obtain white powder of Me₄bpz (**b** in Scheme S1).

Cu(Me₄bpz)₂(NO₃)₂ (Structure 1) In a typical synthesis, a mixture of Cu(NO₃)₂•3H₂O (5.0 mg, 0.021 mmol) and Me₄bpz (7.5 mg, 0.039 mmol) was dissolved in a solution of 2.0 mL *N,N*-dimethylacetamide (DMA) in a 5 mL glass vial. The vial was capped tightly and placed in an oven at 100 °C for 24 h. Light violet single crystals were collected and rinsed with 3 mL DMA 3 times and then 3 mL acetone 6 times. The formula of the framework Cu(Me₄bpz)₂(NO₃)₂ was determined by the single crystal X-ray diffraction.

Zn(Me₄bpz)(SO₄) (Structure 2) A mixture of ZnSO₄•7H₂O (7.4 mg, 0.026 mmol) and Me₄bpz (5.0 mg, 0.026 mmol) was dissolved in a solution of 2 mL DMA in a 5 mL glass vial. The vial was capped tightly and heated at 90 °C for 4 d. Colorless single crystals were collected and rinsed with 3 mL DMA for times. The formula of the structure Zn(Me₄bpz)(SO₄) was determined by the single crystal X-ray diffraction.

Crystal structure determination

The crystal structures were determined by single crystal X-ray diffraction. Data were collected on a

Bruker SMART APEX II X-ray single crystal diffractometer equipped with a CCD area detector with Cu K α radiation ($\lambda=1.54178 \text{ \AA}$) at 173(2) K. The crystal structures were solved by Direct Methods and refined on F^2 by full-matrix least-squares using the SHELXTL-97^[32] program. All non-hydrogen atoms were refined with anisotropic thermal parameters, and all hydrogen atoms were placed in calculated positions.

Unit cell parameters of structure **1**: Tetragonal space group $P42_12$, $a=18.7607 \text{ \AA}$, $c=8.2643 \text{ \AA}$. Unit cell parameters of structure **2**: Monoclinic space group $C2/c$, $a=19.7610 \text{ \AA}$, $b=15.3819 \text{ \AA}$, $c=15.1674 \text{ \AA}$, $\beta=129.435^\circ$.

Results and Discussion

Crystal structure of Cu(Me₄bpz)₂(NO₃)₂

Cu(Me₄bpz)₂(NO₃)₂ crystallizes in the tetragonal space group $P42_12$ with four formula units per unit cell. Each Cu(II) in this MOF structure is in octahedral geometry. In this unit, the equatorial plane is occupied by four nitrogen atoms from four Me₄bpz ligands respectively, while the axial positions are occupied by two oxygen atoms from two nitrates, forming a *trans*-CuN₄O₂ unit (Figure 1a). While in another MOF

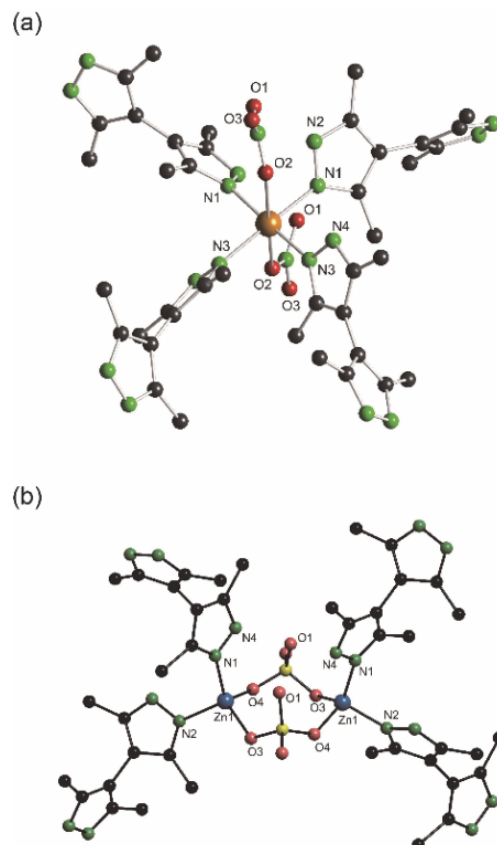


Figure 1 Different coordination environment caused by different anionic ligands. (a) The coordination environment of Cu(II) in **1**. (b) The coordination environment of Zn(II) in **2**. Cu, brown; Zn, blue; N, green; S, yellow; C, black; O, red. Hydrogen atoms are omitted for clarity.

constructed by Cu and Me₄bpz, Cu(Me₄bpz),^[23] Me₄bpz ligand is four-coordinated with four copper atoms by four nitrogen atoms, and four adjacent Cu atoms form a square-shape Cu₄ node. In structure **1**, the bond lengths of Cu1—N1 and Cu1—N3 are 1.97 and 1.99 Å, respectively, which are comparative to those observed in Cu(Me₄bpz). The bond distance of Cu1—O2 is 2.72 Å, the relatively long Cu1—O2 distance indicates the weak coordination between the Cu(II) and the nitrate ion. Careful inspection reveals that the Cu1…N2 and Cu1…N4 distances are 2.89 and 2.91 Å, respectively, and these N atoms from the pyrazoles are quite close to the nitrate ions. The steric hindrance may be the reason why the Cu1—O2 distance is longer than the typical Cu—O bond length.

Each metal is linked by four Me₄bpz ligands with the Cu…Cu distance being 9.46 Å. On the other hand, the ligands are two-connected, in which the two non-hydrogen bearing nitrogen atoms are in the *endo*-positions. This *endo*-bidentate mode of Me₄bpz is comparable with several other MOFs based on the same linker.^[25–27]

The linker and Cu(II) further assemble into an infinite 2D planar network (Figure 2a). These 2D layers in wave-like forms pack along *c*-axis in eclipsed fashion, with the inter-layer distance of 6.70 Å, as measured by the distance between two corresponding Cu ions at neighboring layers (Figure 2b). Inter-layer hydrogen bonds between O in nitrate and the N—H in the pyra-

zole ring ($d(\text{N}—\text{H}\cdots\text{O})=2.85$ Å) along *c*-axis can be found as the packing force of this supramolecular architecture. This MOF structure presents two types of one-dimensional channel: the first channel has a size of 3.0 Å in diameter, and the second type is 2.0 Å in diameter. The relatively narrow pore size is due to the CH₃ and NH groups in Me₄bpz ligand which direct inwards the pores.

Crystal structure of Zn(Me₄bpz)(SO₄)

Zn(Me₄bpz)(SO₄) crystallizes in the monoclinic space group *C2/c* with eight formula units per unit cell. The coordination environment of Zn(II) with atom labeling is shown in Figure 1b. Each Zn(II) is coordinated with two nitrogen atoms from two Me₄bpz ligands respectively and two oxygen atoms from two sulfate groups to form a distorted tetrahedron. Two crystallographically symmetric Zn(II) ions connect through two sulfate groups forming an eight-membered ring, and Zn(II)…Zn(II) distance in this dinuclear SBU is 4.41 Å. The bond distances of Zn—N are 1.91 and 1.98 Å, which are similar to those in Zn(Me₄bpz),^[23] and the Zn—O distances are around 1.94 Å. Similar to structure **1**, the ligand in *endo*-bidentate mode here is also two-coordinated through the two non-hydrogen bearing nitrogen atoms in the pyrazoles.

In line with structure **1**, each SBU connects with four adjacent SBUs by four Me₄bpz ligands along *a*- and *b*-axis to form infinite 2D layer network (Figure 3a). Furthermore, the adjacent layers are packed by hydro-

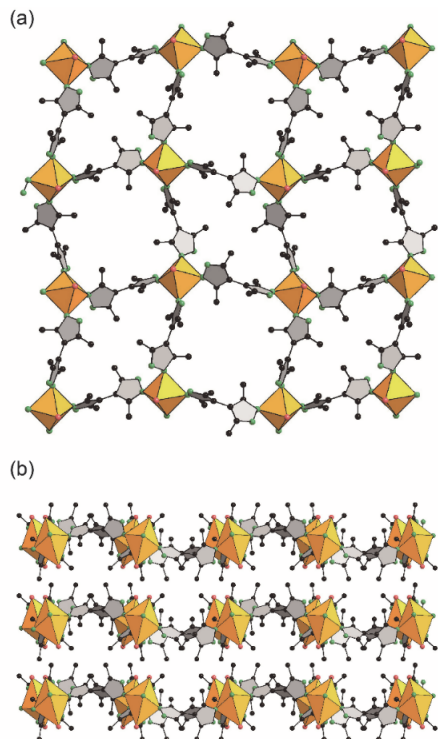


Figure 2 The crystal structure of Cu(Me₄bpz)₂(NO₃)₂ with views along (a) *c*-axis and (b) *a*-axis. SBUs are emphasized by yellow octahedra. Nitrogen atoms are depicted as green spheres, carbon atoms as black spheres, and oxygen atoms as red spheres. Hydrogen atoms are omitted for clarity.

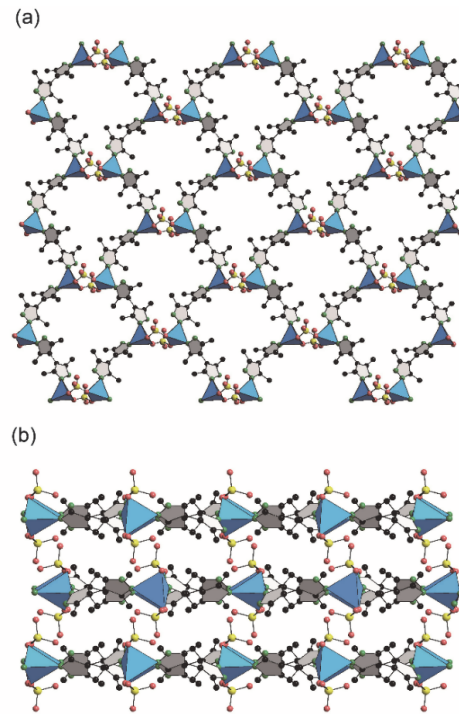


Figure 3 The crystal structure of Zn(Me₄bpz)(SO₄) with views along (a) *c*-axis and (b) *a*-axis. SBUs are emphasized by blue tetrahedra. N, green; C, black; S, yellow; O, red. Hydrogen atoms are omitted for clarity.

gen bonds between O in sulfate groups and the N—H in the pyrazole ring ($d(\text{N}—\text{H}\cdots\text{O})=2.72 \text{ \AA}$) to generate a 3D framework (Figure 3b). The layers stack on top of each other with equal interlayer separation at 7.79 \AA . This framework contains 1D channels along c -axis with the size of 3.0 \AA in diameter.

Metal-anion coordination in the MOF structures

In structure **1**, nitrate group is mono-coordinated to Cu(II) as a terminal ligand; while the bidentate SO_4^{2-} acts as bridging ligand when it is coordinated to Zn(II) in structure **2**, resulting in the formation of binuclear SBU.

Due to the relatively mild reaction conditions employed and the requirement to make the structure neutral, the existence of these ions in the crystal structures is inevitable. We believe that Cu(II) tends to be in the octahedral geometry, and the *trans*-effect of octahedral complex prefers to assign the anions to the two axial positions. The two nitrates far away each other make forming dinuclear SBUs impossible in structure **1**. On the other hand, Zn(II) prefers tetrahedral geometry. When the two sulfates are coordinated to the same Zn(II), they are close to each other. Thus they can act as two bridging ligands to join two Zn(II) together, and the dinuclear SBU was assembled *in situ*. These two structures clearly demonstrate the role of anion participation in the formation of MOFs with distinct structures.

By simplifying the Cu(II) in structure **1** and the dinuclear Zn-based SBU in structure **2** as the nodes and Me₄bpz as linkers, both frameworks have (4,4)-connected networks, and their topology is **sql**.^[33]

Anion-involved hydrogen bonding in the MOF structures

The anions with O donors could also form hydrogen bonds with neighboring organic linkers, thus fine tune the structures of the extended networks. In both structures presented, the anion and the linker are quite close to each other when they are coordinated to the same metal. The two pyrazolate rings in Me₄bpz have a dihedral angle of 66° in structure **1** and around 70° in structure **2**, which are comparative to those observed in other MOFs constructed by Me₄bpz, making the N—H in pyrazole rings pointing to the anions. In structure **1**, the hydrogen bonds between O in nitrate groups and N—H in pyrazole rings ($d(\text{N}2—\text{H}\cdots\text{O}1)=2.751 \text{ \AA}$) were observed. Similarly, in structure **2**, there are hydrogen bonds between O in sulfuric groups and the N—H in the pyrazolate rings ($d(\text{N}4—\text{H}\cdots\text{O}1)=2.612 \text{ \AA}$). These hydrogen bonds between inorganic ionic ligand and the pyrazole ring may be the reason why the linkers are in *endo*-bidentate mode in both structures.

Spectroscopic and thermogravimetric analyses

In the FT-IR spectra, the absorption peaks around 1400 cm^{-1} correspond to nitrate groups in structure **1** (Figure S1), while the absorption peaks around 1100 cm^{-1}

correspond to sulfate groups in structure **2** (Figure S2). The broad absorption bands around 3500 cm^{-1} are associated with N—H stretching vibrations, which proves that NH groups are not deprotonated in both structures. The absorption bands observed at 3000 cm^{-1} correspond to C—H stretching vibrations on the heterocyclic ring, while the C—H in-plane deformations are obtained between 1000 and 1100 cm^{-1} . The absorption bands between 1500 and 1700 cm^{-1} correspond to the ring stretching modes (C=C, N—C and N—N).

The emission spectrum of **2** was examined in the solid state at room temperature (Figure 4). The free ligand Me₄bpz displays emission maxima at 422 nm .^[25] Upon excitation at 370 nm , complex **2** has broad emission band with the maximum intensity at 440 nm in the photoluminescence spectrum. Due to the electrochemical inertness of d¹⁰-configured Zn(II) ion, emission of **2** is ascribed to ligand-centered transitions rather than LMCT or MLCT.^[34] Additionally, compared with other MOFs constructed with Me₄bpz ligand,^[35] the origin of the emission of **2** is considered as an intraligand $\pi^*\text{--}\pi$ transition. The red shift of **2** compared to Me₄bpz is 18 nm , which is attributed to the increase in the rigidity of ligands due to metal–ligand coordination.

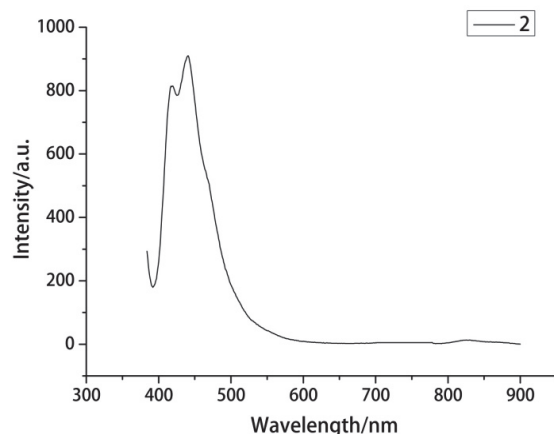


Figure 4 Photoluminescence spectrum of **2** with excitation at 370 nm .

Thermal gravimetric analyses indicate that structures **1** and **2** are stable up to about $250 \text{ }^\circ\text{C}$ (Figure S3), while the previously reported Cu(Me₄bpz) and Zn(Me₄bpz) are stable in air up to $400 \text{ }^\circ\text{C}$.^[23] The lower thermal stability of these two structures is probably caused by NH groups in pyrazoles which are not coordinated to metal ions. In Cu(Me₄bpz) and Zn(Me₄bpz), each Me₄bpz ligand is four-coordinated, while in **1** and **2**, each Me₄bpz ligand is two-coordinated.

Conclusions

Two new two-dimensional MOF structures have been synthesized by employing the methyl functionalized bipyrazole as the organic linker. Both structure **1** [$\text{Cu}(\text{Me}_4\text{bpz})_2(\text{NO}_3)_2$] and structure **2** [$\text{Zn}(\text{Me}_4\text{bpz})_2\text{SO}_4$]

can be described as packing of square grids. Besides the metal-ligand coordination during the MOF assembly, the anions have also participated in the framework construction. The monodentate NO_3^- and the bidentate SO_4^{2-} have created single Cu ions and dinuclear Zn clusters as inorganic SBUs for the MOFs, respectively, due to the metal-inorganic anion coordination. What is more, the anions are also involved in the hydrogen bonds between the anions and the organic linkers, resulting in the *endo*-conformation of the linkers in the MOF structures. These interactions, combined with the major metal-ligand coordination, will produce interesting MOFs with more structural diversity and extraordinary properties in the future.

Acknowledgement

This work was supported by the Education Department of Zhejiang (No. Y201120341).

References

- [1] Li, H.; Eddaoudi, M.; O'Keeffe, M.; Yaghi, O. M. *Nature* **1999**, *402*, 276.
- [2] Kitagawa, S.; Kitaura, R.; Noro, S. *Angew. Chem., Int. Ed.* **2004**, *43*, 2334.
- [3] Férey, G. *Chem. Soc. Rev.* **2008**, *37*, 191.
- [4] Sumida, K.; Rogow, D. L.; Mason, J. A.; Medonald, T. M.; Bloch, E. D.; Herm, Z. R.; Bae, T. H.; Long, J. R. *Chem. Rev.* **2012**, *112*, 724.
- [5] Natarajan, S.; Mahata, P. *Chem. Soc. Rev.* **2009**, *38*, 2304.
- [6] Li, Q.; Zhang, W.; Mijanić, O. Š.; Sue, C.-H.; Zhao, Y.-L.; Liu, L.; Knobler, C. B.; Stoddart, J. F.; Yaghi, O. M. *Science* **2009**, *325*, 855.
- [7] Wang, P.; Kang, M.; Sun, S.; Liu, Q.; Zhang, Z.; Fang, S. *Chin. J. Chem.* **2014**, *32*, 838.
- [8] Su, Z.; Fan, J.; Okamura, T.-A.; Sun, W. *Chin. J. Chem.* **2012**, *30*, 2016.
- [9] O'keeffe, M.; Yaghi, O. M. *Chem. Rev.* **2012**, *112*, 675.
- [10] Corma, A.; Garcia, H.; Xamena, F. X. L. *Chem. Rev.* **2010**, *110*, 4606.
- [11] Ponomarova, V. V.; Komarchuk, V. V.; Boldog, I.; Chernega, A. N.; Sieler, J.; Domasevitch, K. V. *Chem. Commun.* **2002**, *436*.
- [12] Ganesan, P. V.; Kepert, C. J. *Chem. Commun.* **2004**, 2168.
- [13] He, J.; Yin, Y.-G.; Wu, T.; Li, D.; Huang, X.-C. *Chem. Commun.* **2006**, 2845.
- [14] Zhang, J.-P.; Horike, S.; Kitagawa, S. *Angew. Chem., Int. Ed.* **2007**, *46*, 889.
- [15] Zhang, J.-P.; Kitagawa, S. *J. Am. Chem. Soc.* **2008**, *130*, 907.
- [16] Hou, L.; Lin, Y.-Y.; Chen, X.-M. *Inorg. Chem.* **2008**, *47*, 1346.
- [17] He, J.; Zhang, J.-X.; Tsang, C.-K.; Xu, Z.; Yin, Y.-G.; Li, D.; Ng, S.-W. *Inorg. Chem.* **2008**, *47*, 7948.
- [18] Hunger, J.; Krautscheid, H.; Sieler, J. *Cryst. Growth Des.* **2009**, *9*, 4613.
- [19] Lin, L.; Yu, R.; Yang, W.; Wu, X.-Y.; Lu, C.-Z. *Cryst. Growth Des.* **2012**, *12*, 3304.
- [20] Pettinari, C.; Tabacaru, A.; Boldog, I.; Domasevitch, K. V.; Galli, S.; Masciocchi, N. *Inorg. Chem.* **2012**, *51*, 5235.
- [21] Sun, Y.-Q.; Deng, S.; Liu, Q.; Ge, S.-Z.; Chen, Y.-P. *Dalton Trans.* **2013**, *42*, 10503.
- [22] Du, L.-Y.; Shi, W.-J.; Hou, L.; Wang, Y.-Y.; Shi, Q.-Z.; Zhu, Z. *Inorg. Chem.* **2013**, *52*, 14018.
- [23] Tăbăcaru, A.; Pettinari, C.; Timokhin, I.; Marchetti, F.; Casrasco-Mařín, F.; Maldonado-Hódar, F. J.; Galli, S.; Masciocchi, N. *Cryst. Growth Des.* **2013**, *13*, 3087.
- [24] Han, L.-L.; Zhang, X.-Y.; Chen, J.-S.; Li, Z.-H.; Sun, D.-F.; Wang, X.-P.; Sun, D. *Cryst. Growth Des.* **2014**, *14*, 2230.
- [25] Tomar, K.; Rajak, R.; Sanda, S.; Konar, S. *Cryst. Growth Des.* **2015**, *15*, 2732.
- [26] Xu, Z.; Han, L.-L.; Zhuang, G.-L.; Bai, J.; Sun, D. *Inorg. Chem.* **2015**, *54*, 4737.
- [27] Boldog, I.; Rusanov, E. B.; Chernega, A. N.; Sieler, J.; Domasevitch, K. V. *J. Chem. Soc., Dalton Trans.* **2001**, 893.
- [28] Boldog, I.; Rusanov, E. B.; Chernega, A. N.; Sieler, J.; Domasevitch, K. V. *Angew. Chem., Int. Ed.* **2001**, *40*, 3435.
- [29] Stork, N.; Biswas, S. *Chem. Rev.* **2012**, *112*, 933.
- [30] Mosby, W. L. *J. Chem. Soc.* **1957**, *79*, 3997.
- [31] Boldog, I.; Rusanov, E. B.; Chernega, A. N.; Sieler, J.; Domasevitch, K. V. *Polyhedron* **2001**, *20*, 887.
- [32] Sheldrick, G. M. *Acta Crystallogr.* **2008**, *A64*, 112.
- [33] O'Keeffe, M.; Peskov, M. A.; Ramsden, S. J.; Yaghi, O. M. *Acc. Chem. Res.* **2008**, *41*, 1782.
- [34] Walkup, G. K.; Burdette, S. C.; Lippard, S. J.; Tsien, R. Y. *J. Am. Chem. Soc.* **2000**, *122*, 5644.
- [35] He, J.; Zhang, J.-X.; Tan, G.-P.; Yin, Y.-G.; Zhang, D.; Hou, M.-H. *Cryst. Growth Des.* **2007**, *7*, 1508.

(Pan, B.; Qin, X.)